International Journal of Chemical Engineering and Applications, Vol. 1, No. 1, June 2010
ISSN: 2010-0221

Molecular Dynamic Simulation of Multilayer Methane Adsorption on/in Open Ended Single-Walled Carbon Nanotubes

S.Shokri[1], R.Mohammadikhah[2], H. Abolghasemi[3], A. Mohebbi[4] , H. Hashemipour[5], M. Ahmadi-Marvast[6] and Sh. Jafari Nejad[7]

Abstract— **In this paper, methane adsorption on open ended single-walled carbon nanotubes (o-SWCNT) is studied using molecular dynamics simulation. A site-site potential model of so-called Leonard-Jones is considered to evaluate all interactions. Monolayer/multilayer adsorption isotherms for methane inside/outside of an armchair (10, 10) o-SWCNT are obtained at different temperatures. The simulation data are compared with those of the classical adsorption models. Among the many isotherms tested for the monolayer data, we found that the hybrid isotherm model of the Langmuir and Sips with four parameters nicely fitted the simulation data. The isosteric heat of adsorption is measured as well. Capillary condensation for multilayer adsorption is detected on the mezzo pores at 70 and 170 K.**

Index Terms—**Adsorption, Surface coverage, Isosteric heat, Langmuir equation, Monolayer, Multilayer, Sips equation.**

I. Introduction

Demand for clean fuels for vehicles of coal and petroleum has been rapidly increasing with the development and progress of modern civilization. In this regard, hydrogen and natural gas, whose main component is methane, are commonly considered to be suitable non-pollution alternatives to fossil fuel. Hence, the storage of natural gas has become an important subject. Generally, heavy steel cylinders stores the compressed natural gas under pressures up to 30 Mpa while adsorbed natural gas requires a lower pressure (e.g. about 4 Mpa) to be stored in a lightweight container. Compared to the compressed natural gas, adsorbed natural gas is a very promising because storage in lower pressures leads to lower cost and weight of fuel [1-3]. Recently, there has been a resurgence of interest in potential of carbon materials as gas storage media following claims that single-walled carbon nanotubes, SWCNTs, may have high gas storage capacities. Besides, another possible way of methane exportation can inexpensively be developed via such an adsorptive strategy. For these reasons, the methane adsorption process deserves to be more and more known. Experimental investigation of methane adsorption on closed ended single-walled carbon nanotube bundles has been carried out by Talapatra et al. [4]. Grand canonical Monte Carlo simulations with a Leonard-Jones potential have been performed to study the adsorption of methane at room temperature on triangular arrays of SWCNT [5]. Adsorption of methane on an isolated SWCNT has been investigated so as to increase the volumetric capacity [6]. Kaneko and co-workers have also been studied the methane adsorption process on SWCNT using a density functional theory method [7]. They found that SWCNT with disordered structure could be applied as storage media for methane and other supercritical gases. Information about self-diffusivity of methane obtained from a classical molecular dynamic (MD) simulation at sub- and supercritical conditions is available [8]. To our knowledge, to date there have been no studies about investigation of the classical models for this particular process. In general, there have been a few reports on the adsorption of methane on the surface of SWCNT by means of both experiments and MD simulations. In this paper, methane adsorption on/in (10, 10) SWCNTs is probed at different temperatures and pressures using molecular dynamic simulations. Surface coverage for both exohedral and endohedral associated with isosteric heat is reported. Finally, the simulation data are correlated with some of the classical adsorption models looking for a suitable model for prediction of adsorption capacity.

Research Institute of Petroleum Industry, Tehran, Iran
School of Chemical Engineering, Faculty of Engineering, the University of Tehran, Tehran, Iran
Chemical Engineering Department, Faculty of Engineering, Shahid Bahonar University of Kerman, Iran
Corresponding author. Tel.:+9848252503; fax:+982144739713(e-mail address: shokris@ripi.ir).

II. Method

MD calculations are carried out in the NVT ensemble by a new code written in the FORTRAN77 software environment. Both carbon atoms and methane molecules are treated as spherical rigid bodies. Pairwise interactions between fluid-fluid and fluid-surface are modeled with Leonard-Jones potential. This potential is define as below:

$$U^{lj} = 4\varepsilon\left[\left(\frac{\sigma}{r}\right)^{12} - \left(\frac{\sigma}{r}\right)^{6}\right] \quad (1)$$

Where r is the separation distance between two individual bodies. The energy and size parameters of the LJ potential are ε_f =148.12 K, σ_f =3.81 Å for methane-methane interactions and ε_f =28 K, σ_f =3.35 Å for carbon-carbon interactions [9]. Lorentz-Bertholet combining rule is used for estimation of fluid-surface interactions in this form [10]:

$$\sigma_{sf} = \frac{\sigma_f + \sigma_c}{2} = 3.58 \text{ Å} \quad (2)$$

and

$$\varepsilon_{sf} = \sqrt{\varepsilon_c \varepsilon_f} = 64.4 \text{ K} \quad (3)$$

A perfect (10, 10) SWCNT with opened ends, is chosen

as absorbent. Fig.1 is showing our substrate enclosed by a fictitious cubic box. Each unit of cell of the (10, 10) SWCNT comprises 40 carbon atoms with the radius and length of 6.78 Å and 2.46 Å, respectively. The substrate included 1520 carbon atoms corresponding to 38 unit cells duplicated along the tube axis. The substrate is enclosed by a cubic box of 95.2×95.2×95.2 $Å^3$ (simulation box) as one can see in Fig.1 where the c-c bond length through the absorbent is about 1.42 Å. The number of methane molecules in the simulation box varied between 32 and 6912 molecules. Since in MD the large intermolecular potentials and the correspondingly large forces could cause difficulties in the solution of the stiff differential equations of motion, the initial configuration of methane molecules has been organized according to the face-centered cubic (fcc) structure with its $4M^3$ $(M = 2,3,4,5,...)$ lattice points. Our code incorporated an important section through which all overlaps between methane molecules and surface were eliminated until the maximum distance between fluid molecules and SWCNT is less than $0.8\sigma_{sf}$. This action avoids large-scale interactions. Initial linear momentums (velocities) were set by a random generation Monte Carlo method, which was satisfying the principle of total momentum conservation. Initial angular momentums were taken as zeroes, so the momentum conservation rule becomes:

$$P = \sum_{i=1}^{N_f} m_i v_i = 0 \quad (4)$$

A Woodcock extended system thermostat is used to rescale the velocities for fixing the kinetic temperature of the system [13]. The way is that at each time step the velocities are multiplied by a factor of $(T/T_{curr})^{1/2}$, where T is the desired thermodynamic temperature and T_{curr} is the current kinetic temperature. The fixed carbon atoms are not included in the calculation of temperature.

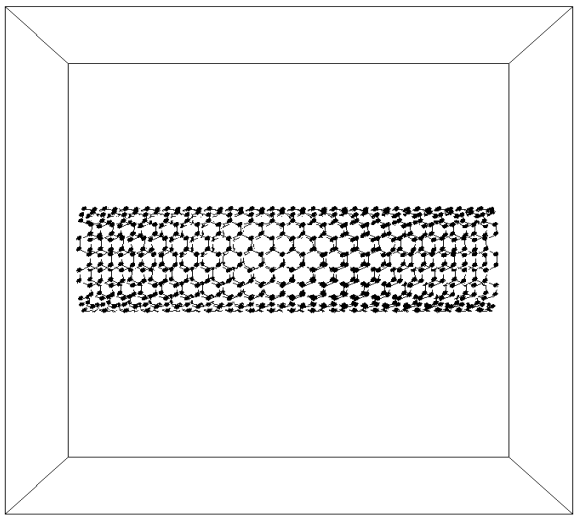

Fig.1: Computer-generated image of an armchair (10, 10) SWCNT.

The 3-D periodic boundary conditions were imposed on methane molecules so as to vanish the surface effect of the box faces. The LJ potential model is truncated for the Vander Waals cutoff that is chosen 12.8 Å, therefore, any interaction related to farther distance is assumed to be negligible. The system is equilibrated for 1200 ps and the ensemble averages of properties of interest are evaluated and stored during simulation. The relaxation of initial configuration to equilibrium evolves 120000 time steps. No studies in MD have reported such long time simulation because of some limitations of computer systems in addition to molecular modeling packages. However, the simulation procedure will certainly be bothersome if user uses the usual MD packages. Conversely, the use of manual codes is more convenience to handle various problems but more difficult to write. We optimized the integration time, the main section, of our program and could proceed the simulation procedure to long times. This action gives us results that are more reliable. The equations of motion in the form of Hamiltonian are integrated by the Varlet's algorithm when the time step is short enough as 1 fs [11]. The ensemble averages obtained from simulations are taken into account for secondary analysis. A new program was linked to the main program for subsequent calculations. The uncertainties on the ensemble averages are calculated by repeated simulations and estimated to be less than 2%. Convergence history for dimensionless total/potential energy during simulation of 500 methane molecule until 20000 time steps (20 ps) is shown in Fig.2, where it is clear that after 8000 time steps (8ps) the system gets the equilibrium state. If the number of total carbon and methane molecules increase, the equilibrium time exponentially increases. For a specified simulation, dimensionless pressure and temperature should be hold constantly although they change frequently around their setting values (Fig.3).

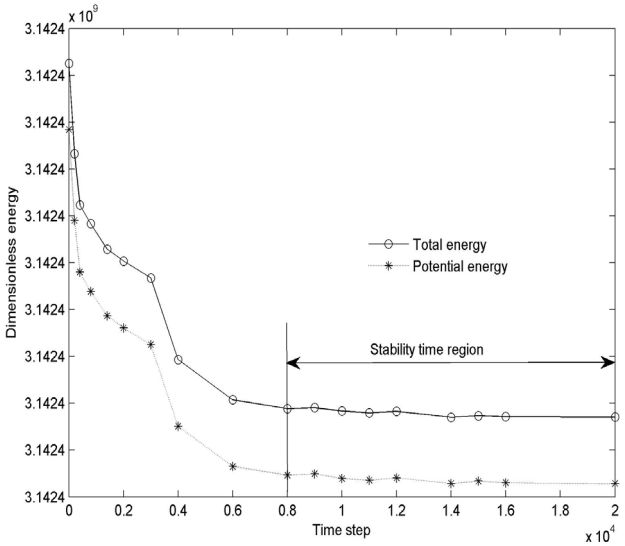

Fig.2: Convergence history of dimensionless energy during simulation of 500 methane molecules.

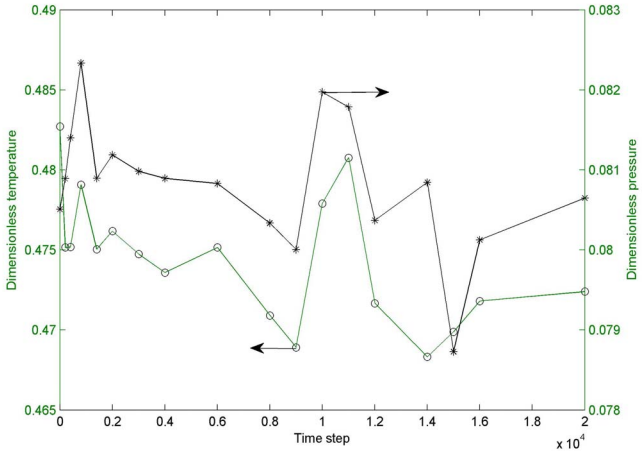

Fig.3: Convergence history of dimensionless temperature and pressure for simulation of 500 methane molecules.

III. Results and Discussion

A. Monolayer coverage on o-SWCNT

This fact has been recognized that methane is weakly adsorbed on/in CNTs even under very high pressure (i.e. the interaction between methane-CNT is of small degree of magnitude) [15]. Results show at low pressure, a symmetrical monolayer of methane molecules is constituted around and inside of CNT. When the pressure increases, the second, third, fourth and higher layers are formed around CNT successively while inside of CNT there is only one layer. The pressure increase is equivalent to increase in methane molecules in the box. Fig.4 shows a 2-D snapshots of methane adsorbed on/in SWCNT compared to its initial configuration where the number of methane molecules, kinetic temperature and average pressure are 4000, 70 K and 3.89 Mpa, respectively. In this case, the system reaches the liquid state. From this figure, it is clear that the first, 2nd and 3rd layers are nearly complete but the higher levels are incomplete.

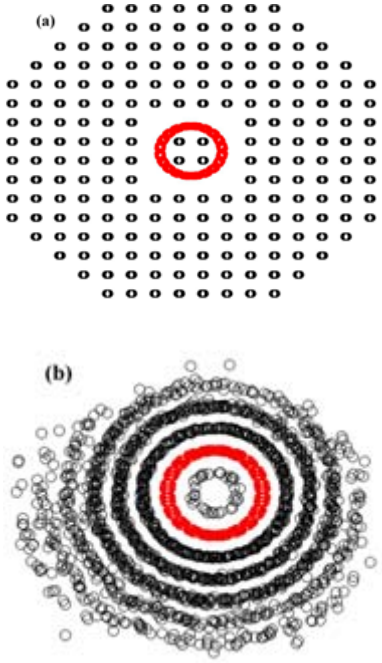

Fig.4: Two dimensional snapshots of (a) initial (fcc) and (b) equilibrium configurations.

The simulations are performed at different temperatures as 70, 170, 273 and 298 K under which temperatures the surface coverage changes very sensitively against the temperature variation. For example, at 298 and 273 K only monolayer is formed when the further layers are vanished. This fact is related to the increases in kinetic energy in contrast with potential energy, which is responsible for surface adsorption. The total energy, Hamiltonian, are conserved during the system evolution as long as the algebraic summation of kinetic and potential is identical to zero. In the other words, increase in kinetic energy results decrease in potential energy and vice versa. The mathematical aspect of this law is:

$$H = U + K = 0 \tag{5}$$

Where H, U and K are total (Hamiltonian), potential and kinetic energies, respectively. Consequently, increases in temperature indeed decrease surface coverage. At each time step, Eq.5 has to repeatedly be checked to prevent divergence. The equilibrium distance between the CNT wall and the first monolayer of methane was spanned as 3.33 Å while for internal layer it was 3.48 Å. The internal distance is found to be higher than the external distance because of the counter interactions induced by carbon atoms in the opposite site of wall. Surface coverage of methane adsorption is expressed in terms of atomic ratio of adsorbed methane to carbon by Eq.6.

$$\theta = \frac{N_m}{N_c} \tag{6}$$

That N_m stands for the number of methane molecules adsorbed on the substrate. This property may also be expressed in either volumetric or mass unit, although the atomic unit is the best choice due to its high accuracy. Surface coverage at four different temperatures is calculated under several pressures, as one can see in Fig.5. The average pressure is integrated over its instantaneous values divided to the number of time steps.

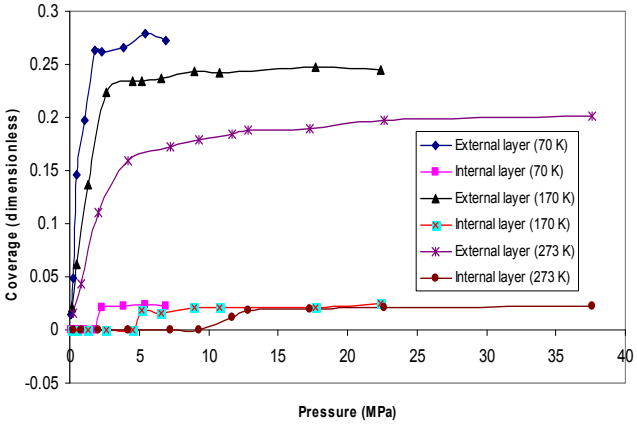

Fig.5: Coverage of methane adsorption on the external and internal surface of the (10, 10) o-SWCNT at different temperatures.

Saturation coverage for 70, 170, 273 and 298 K are directly evaluated with counting the adsorbed molecules under high pressures and for the first external layer find to be 0.278, 0.248, 0.201 and 0.197 while for internal layer the corresponding values are 0.0253, 0.0250, 0.0230 and 0.0217, respectively.

Fig.4. (a) showing that there are initially four columns of methane molecules confined inside the (10, 10), after equilibrium, methane molecules take a 2D cubic configuration. By increasing internal coverage, this structure changes from previous to a 2D hexagonal one and subsequent proceeding gives a 2D gyrate form. This fact is also observed for external layers but less sensible.

B. Investigation of models

In this section, some of typical adsorption models whether theoretical or experimental, namely Langmuir, Sips, Freundlich and Langmuir-Sips, are correlated with the simulation data. The relations of these models accompanied by more details about can be found elsewhere [12]. For instance, the hybrid isotherm of Langmuir-Sips is defined beneath:

$$\theta = q_m\left(\frac{b_L p}{1+b_L p}+\frac{b_S p^{1/n}}{1+b_S p^{1/n}}\right) \quad (7)$$

Where θ, the fractional coverage, is the ratio of unsaturated coverage to the full capacity of under consideration layer and p is the mean pressure of the system. Subscripts L and S denote on their belonging to the Langmuir and Sips equation, respectively. The parameters b, n and q_m at specified temperature are constant values having only material dependency. Prior to start analysis, some of the doubtful simulations were repeated. Eventually, the data were carefully looked over and some of the adverse data points were rejected. However, the hybrid isotherm of Langmuir-Sips, capable of explaining the coverage of both internal and external layers, was superior to flexible fit of isotherm data than others although its physical meaning is arguable. Results for monolayer methane adsorption at 70 K are shown in Fig.4 from which the excellent agreement between the hybrid model and the data is evident. This conclusion is thoroughly consistent with that obtained from analysis on experimental data [2].

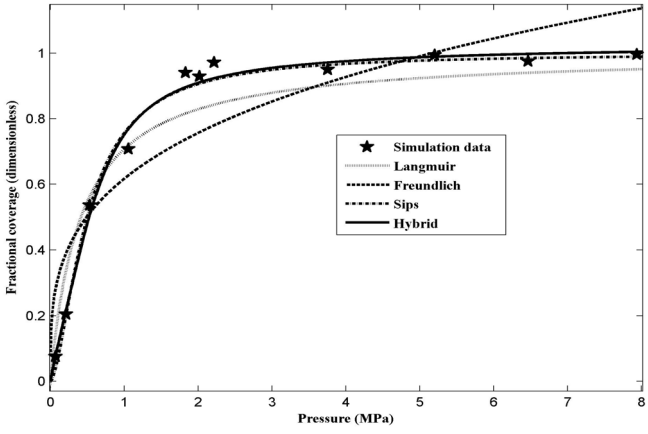

Fig.6: Correlation between common models and simulation data at 70 K. The values of R-square for Langmuir, Freundlich, Sips and hybrid isotherms are 0.939, 0.802, 0.989 and 0.992, respectively.

Henceforth, our attention will be focused on this isotherm because of its high accuracy. Four parameters of the hybrid model were determined by a nonlinear least squares fitting routine of the Nelder-Mead simplex method done in MATLAB software curve fitting toolbox environment. Adjusted R-square is calculated for fit plots as a criterion of precision. To better understanding of coverage behavior at different temperatures, the fitting procedure was continued, unceasingly. A comprehensive report of the outcome of the fitting is incorporated in Table.1. To our knowledge, such results are being reported for the first time since there has not been any similar work in the literature. The Langmuir-Sips parameters for methane adsorption on MWCNTs just corresponding to the external monolayer are available [2]. It is observable from Table.1 that all parameters change with temperature, erratically. The temperature functionality of the parameters will be unknown in that the number of data point is poor, so the curve fitting is inappropriate. The only way of finding the parameters should be the interpolation between the present data. If a theoretical definition is accessible, the functionality can be known. For example, the temperature dependency of b_L or b_S is hypothetically presented by this equation [12]:

$$b_L = b_0 \exp(-\frac{E_{ads}}{RT}) \quad (8)$$

Where b_0 , R and E_{ads} are pre-exponential factor, universal gas constant and activation energy of adsorption. Eq.8 is valid for Langmuir or Sips equation, discretely, but in combination, the separation contributions of Langmuir and Sips are not transparent. We found that Table.1 and the data therein do not satisfy Eq.8 anyway. This fact is good evidence to previous claim about unknown relation between Eq.7 and Eq.8.

TABLE1: THE PARAMETERS OF LANGMUIR-SIPS EQUATION (EQ.7) IN VARIOUS TEMPERATURES.

Layer to be studied	Temperature (K)	b_L	b_S	n	q_m	Adjusted R-squared
Internal	70	0.034	3.57E-8	0.039	0.757	0.947
	170	0.017	2.29E-8	0.091	0.720	0.914
	273	2.764E-12	2.31E-7	0.160	0.970	0.949
	298	0.010	3.07E-7	0.127	0.751	0.920
External monolayer	70	1.958	3.702	0.405	0.522	0.987
	170	1.602	0.127	0.150	0.503	0.999
	273	0.388	0.331	0.448	0.512	0.998
	298	0.404	0.269	0.882	0.517	0.988

The thought is the essence of Eq.7 probably is different from its composer equations such as Langmuir or Sips.

C. Isosteric heat

One of the basic quantities in adsorption studies is the isosteric heat, q_{st} , which is the ratio of the infinitesimal change in the adsorbate enthalpy to the infinitesimal change in the amount adsorbed. The information of heat released is important in the kinetic studies because when heat is released due to adsorption, the released energy is partly absorbed by the solid adsorbent and partly dissipated to the surrounding. The portion absorbed by the solid increases the particle temperature and it is this rise in temperature that

slows down the adsorption kinetics because the mass uptake is controlled by the rate of cooling of the particle in the later course of adsorption. Hence, the knowledge of this isosteric heat is essential in the study of adsorption kinetics. The isosteric heat may or may not vary with loading. It can be determined from the slope of the plot of *lnp* versus *1/T* for a fixed amount of gas adsorbed on the substrate and is given by Eq.9.

$$q_{st} = -R\left(\frac{\partial \ln p}{\partial 1/T}\right)_{\theta} \tag{9}$$

Variations of *lnp* with *1/T* for both external and internal locations are depicted in Fig.7. The figure is presenting that the slope of the supposed straight lines is unexceptionably negative thus the isosteric heat of adsorption takes positive values in this particular case. The isosteric heat of endohedral and exohedral adsorption of methane as a function of coverage is also illustrated as one can see in Fig.8. As a consequence, this figure shows that isosteric heat of endohedral adsorption follows a piecewise manner whereas exohedral heat is fully continuous. Surprisingly, the endohedral plot shows two sharp peaks; the tallest is in vicinity of coverage of 0.02, which declines rapidly with increase in amount of coverage. Prevalently, the adsorption process is of great interest to be carried out in descending region (i.e. after the tallest peak) because the maximum amount of coverage and minimum generation of heat of adsorption is coincidently reached. For external layer, this treatment is not found.

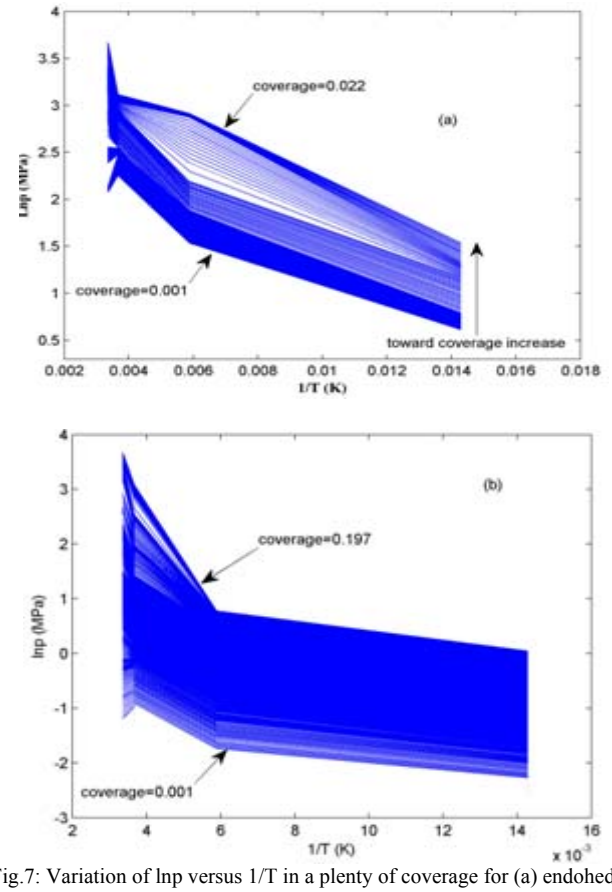

Fig.7: Variation of lnp versus 1/T in a plenty of coverage for (a) endohedral and (b) exohedral adsorption.

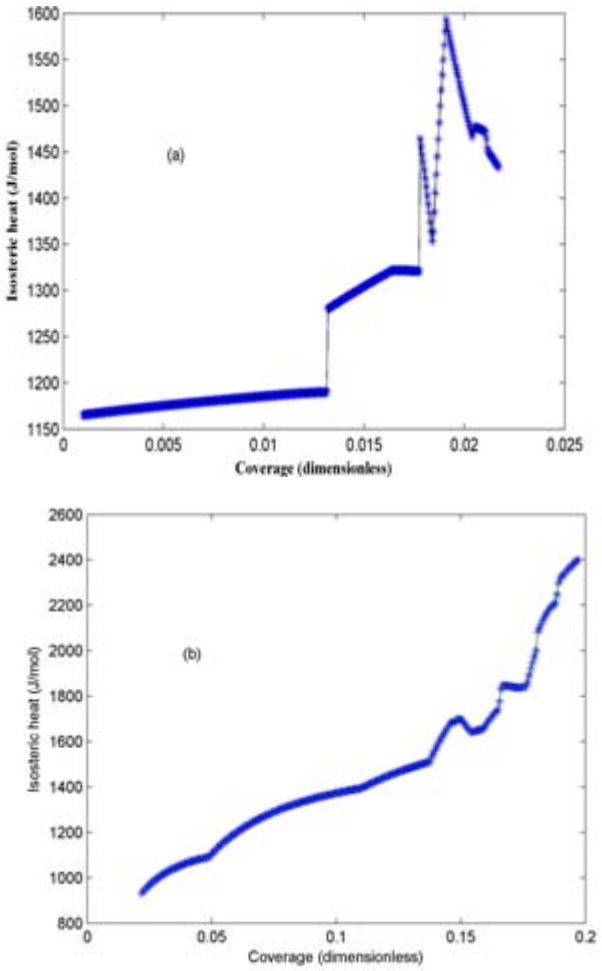

Fig.8: Variation of isosteric heat against coverage for (a) endohedral and (b) exohedral adsorption.

Fig.8. (b) reveals that the exohedral isosteric heat increases with the coverage increase due to attractive interacting with neighbor molecules. If we had taken the higher amount of coverage into calculation, a maximum value of exohedral isosteric heat would surely have obtained due to repulsive forces among adsorbed molecules.

D. Multilayer coverage on o-SWCNT

Multilayer adsorption shows different behavior from the monolayer adsorption due to additional affecting phenomena like capillary condensation, layers overlapping and etc. From this view point, tracing adsorbate molecules in a multilayer adsorption will be difficult. The fact that a specified molecule through which layer is adsorbed, takes much effort than when just a monolayer for adsorption there exists. Generally, the adsorption capacity increases from first layer to second layer and so forth. As Fig.9 showing, the third external layer does not follow this procedure likely due to overlap with the second and forth layers. In fact, adatoms in this layer have lower attraction energy than first and second layer due to its greater distance from the SWCNT surface. Therefore, with a pressure increase, the layer becomes more and more condensed until at the pressure near 4 MPa the repulsive forces overcome inter-molecule attractions. Again, extra pressure increase results in capacity enhancement. Capillary condensation as one of the most important adsorption phenomena occurs at 2 MPa

for isotherm of 70 K, as Fig.10 showing. This phenomenon, with an ascending jump in the plot of variation of total coverage versus pressure, increases dramatically the total adsorption capacity in mezzo pores. Results show that capillary condensation takes place only for 70 and 170 K isotherms at pressures near 2 and 7 MPa. Isotherms for each layer at different temperatures are separately shown below. As one can see in Fig.11, the first internal and external layers are full, where the second and third layer can adsorb more methane molecules with pressure increase. Fig.10 shows that optimal pressure for methane adsorption at 70 K is about 7 MPa under which the adsorption capacity would be full. It is important to conduct the adsorption process under such optimal pressures for energy saving. The total coverage corresponding to temperatures up to 70 K show that a capacity enhancement for process is possible as yet since this pressure remains for maximum total coverage identical to 1 (Fig.11). However, inside of SWCNT essentially one layer is formed and no more because of space prohibition.

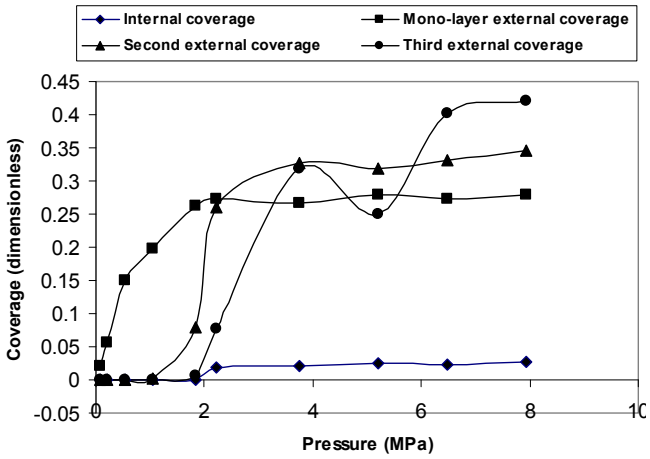

Fig.9: Coverage of multilayer methane adsorption on the external and internal surface of the (10, 10) o-SWCNT at 70 K.

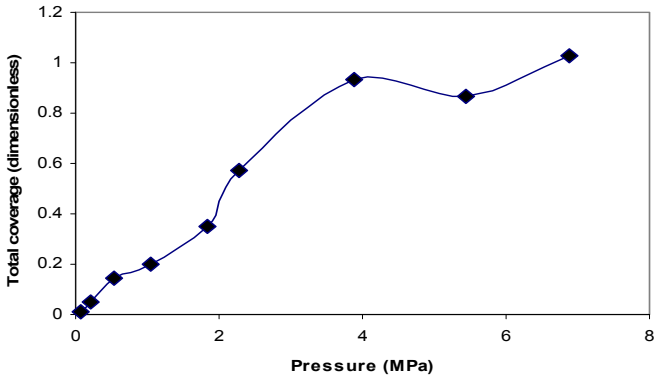

Fig.10: Total coverage of multilayer methane adsorption at 70 K.

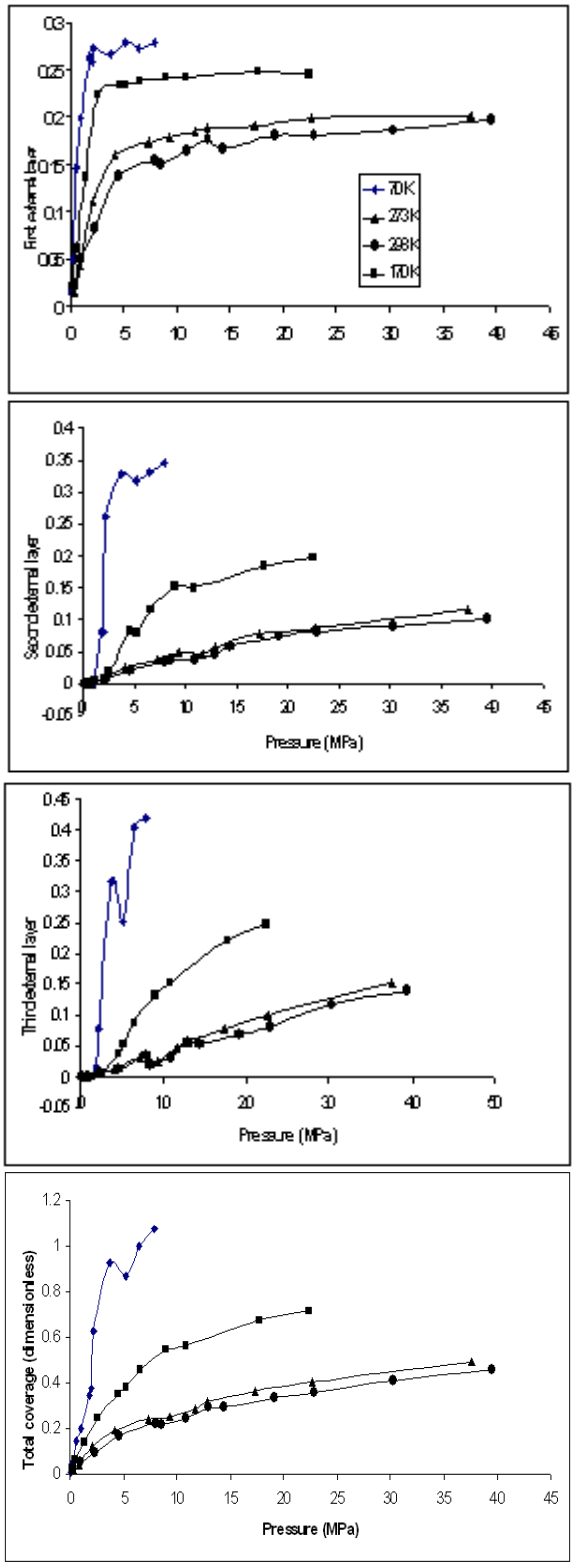

Fig.11: Coverage of multilayer methane adsorption at different temperatures.

E. Investigation of models for multilayer

Table.2 shows the results obtained for multilayer adsorption data when they are correlated with Eq.7. For instance, result of fitting is graphically illustrated in Fig.12 for total coverage (last row of Table.2).

TABLE 2. THE PARAMETERS OF LANGMUIR-SIPS EQUATION (EQ.7) IN VARIOUS TEMPERATURES FOR MULTILAYER ADSORPTION

Layer to be studied	Temperature (K)	b_L	b_S	n	q_m	Adjusted R-squared
Second external layer	70	0.0152	6.357E-5	0.0713	0.8825	0.9985
	170	0.0174	8.420E-4	0.3479	0.7752	0.9907
	273	0.0036	0.02567	0.8416	1.2910	0.9877
	298	0.0273	3.814E-5	1.6240	1.9470	0.9816
Third external layer	70	4.158E-7	2.448E-3	0.1834	0.9879	0.9972
	170	4.824E-6	5.871E-3	0.4448	1.1430	0.9972
	273	9.797E-3	1.035E-5	1.3820	3.4180	0.9532
	298	3.210E-6	4.949E-3	0.7941	2.9680	0.9789
Total layers	70	0.5141	1.695E-4	0.0879	0.5199	0.9867
	170	0.3257	2.958E-2	0.5912	0.5759	0.9987
	273	0.0109	0.1491	1.2430	0.9707	0.9902
	298	0.0074	0.1179	1.2500	1.0830	0.9965

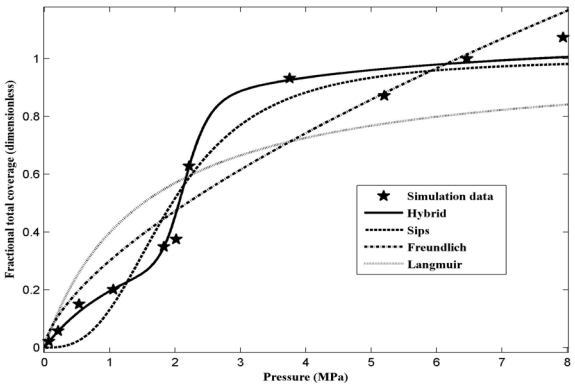

Fig.12: Correlation between common models and simulation data at 70 K.

Once more, hybrid isotherm is more flexible to fitting the simulation data.

IV. CONCLUSION

Methane adsorption on/in SWCNTs is studied at different temperatures as well as pressures. The MD simulations are conducted in NVT ensemble (canonical ensemble) considering molecules as rigid bodies. LJ model is selected to predict all site-site interactions and energy and size parameter are estimated by LB mixing rule. Hamiltonian equations of motion are solved according to the Verlet's algorithm for a long duration of time. Partition function and pressure of the system are evaluated as well. Surface coverage for both internal and external monolayer is directly calculated. It is found that methane molecules are weakly adsorbed on CNT. As a result, the coverage increases with pressure increase while decrease with temperature increase. The simulation data conform to those of predicted by the hybrid isotherm of Langmuir-Sips model. The parameters of the Langmuir-Sips model are obtained via fitting on the simulation data. Finally, the isosteric heat of methane adsorption is studied and it is found that this quantity increases firstly with increase in amount of coverage and decreases, afterwards. Multilayer data of adsorption shows good agreement with that produced by hybrid isotherm. Capillary condensation for multilayer adsorption is found only for temperatures below 170 K. Capillary pressures relative to 70 and 170 K isotherms are found to be 2 and 7 MPa, respectively. The internal space of SWCNT does not allow adsorbate to form capillary condensation because of space prohibition. This phenomenon occurs only at low temperatures on the mezzo pores. Micro and macro pores are not capable of supporting such phenomenon. Our next work will be centralized on multilayer methane adsorption on/in multi-walled carbon nanotubes (MWCNTs).

ACKNOWLEDGMENT

The authors would like to thank Prof A. Nasehzadeh, from the Chemistry Department, Faculty of Science, Shahid Bahonar University of Kerman, Kerman, Iran for helpful discussions.

REFERENCES

[1] H. Tanaka, M. E. Merraoui, W. A. Steele, K. Kaneko, "Methane adsorption on single-walled carbon nanotube: a density functional theory model," *J. Chem. Phys. Lett.,* 352, 2002**,** 334-341.
[2] J. W. Lee, H. C. Kang, W. G. Shim, C. Kim, H. Moon, "Methane adsorption on multi-walled carbon nanotube at (303.15, 313.15, and 323.15) K," *J. Chem. Eng. Data.,* 51, 2006, 963-967.
[3] D. Castello, J. Monge, M. A. de la Lillo, D. Amoros, A. Solano," Advances in the study of methane storage in porous carbon nanotube materials,' *J. Fuel.*, 81, 2002, 1777-803.
[4] S. Talapatra, A. D. Migone, "Adsorption of methane on bundles of closed-ended single-walled carbon nanotubes," *J. Phys. Rev. B.*, 65, 2002, 1-6.
[5] D. Cao, X. Zhang, J. Chen, W. Wang, J. Yun, "Optimization of single-walled carbon nanotube arrays for methane storage at room temperature," *J. Phys. Chem. B.*, 107, 2003, 13286-13292.
[6] E. Bekyarova, K. Murata, M. Yudasaka, D. Kasuya, S. Iijima, H. Tanaka, H. Kahoh, K. Kaneko, "Single-wall nanostructured carbon for methane storage," *J. Phys. Chem. B.*, 107, 2003**,** 4681-4684.
[7] H. Tanaka, El. Merraoui, W. A. Steele, K. Kaneko, "Methane adsorption on single-walled carbon nanotube: a density functional theory model," *J. Chem. Phys. Lett.*, 352, 2002**,** 334-341.
[8] D. Cao, J. Wu, "Self-diffusion of methane in single-walled carbon nanotubes at sub- and supercritical conditions," *J. Langmuir.*, 20, 2004**,** 3759-3765.
[9] W. Shi, J. K. Jahnson, "Gas adsorption on heterogeneous single-walled carbon nanotube bundles," *J. Phys. Rev. Lett.*, **91,** 2003**,** 1-4.
[10] M. P. Allen, T. J. Tildesley, *Computer simulation of liquids*. Clarendon Press, Oxford, 1990.
[11] D. Frenkel, B. Smith, *Understanding molecular simulations: from algoritms to applications*. Academic Press, New York, 1996.
[12] D. D. Do, *Adsorption analysis: equilibria and kinetics*. Imperial College Press, Vol.2, London, 1998.